Available online at www.sciencedirect.com
SCIENCE DIRECT®
Journal of Nuclear Materials 329–333 (2004) 953–957
journal of nuclear materials
www.elsevier.com/locate/jnucmat

Impact of irradiation on the microstructure of nanocrystalline materials

N. Nita [a,*], R. Schaeublin [b], M. Victoria [b]

[a] Institute for Material Research, Tohoku University, Katahira 2-1-1, Aoba-ku, Sendai 980-8577, Japan
[b] Fusion Technology – Materials, CRPP – EPFL, Association EURATOM – Confédération Suisse, 5232 Villigen PSI, Switzerland

Abstract

Nanostructured materials should present a good resistance to irradiation because the large volume fraction of grain boundaries can be an important sink for radiation-induced defects. The objective of the present study is to experimentally investigate the irradiation impact on the microstructure in nanostructured materials. Nickel and Cu–0.5A_2O_3 specimens were synthesized by electro deposition (ED) and severe plastic deformation (SPD). 590 MeV proton irradiation was conducted in the Proton IRradiation EXperiment facility (PIREX). ED Ni were also irradiated in Tandem type accelerator with Ni^+ ions of 840 keV. The irradiation induced microstructure, which leads to hardening, consists exclusively of stacking fault tetrahedra. Their density appears much lower than in the case of coarser grained material. In order to assess the change in grain size induced by irradiation, annealing experiments have been performed. These results, experimentally showing the resistance of nanostructured material to radiation damage, are presented here.

1. Introduction

Nanocrystalline materials have been extensively researched because of their promising properties [1]. Most of these improvements relate to the volume fraction of interfacial regions that increases as the grain size decreases to the nanometer range. On the other hand, it is very important to develop materials highly resistant to intense irradiation fluxes in the frame of the development of future fusion reactors. It is well known that the induced point defects and their clusters can migrate and annihilate at the interfaces of materials. Nanostructured materials should present a good resistance to irradiation because the large volume fraction of grain boundaries can be an important sink for radiation-induced defects. A few experimental studies have been reported about radiation effects on nanocrystalline materials, which suggest a good resistance against irradiation [2,3]. On the simulation side, Samaras et al. [4] performed computer simulations of displacement cascades in nanocrystalline Ni that indicate that the grain boundary acts as an interstitial sink and that a vacancy dominated defect structure remained after solidification of cascade events. Apparently, and even though these materials present an unprecedented potential, knowledge is scarce on the radiation effects on nanocrystalline materials. A detailed microstructural study using known materials in radiation effects is needed.

The objective of the present study is to experimentally investigate the irradiation impact on nanostructured pure metals. Copper and nickel are chosen because they are commonly used as model face centered cubic metals in studies of radiation effects. In the present work, copper strengthened by A_2O_3 particles was examined instead of pure copper because of the added interest of studying grains stabilized by reinforcing particles [5].

2. Experimental procedures

Nanocrystalline Ni and Cu–0.5A_2O_3 samples were prepared by severe plastic deformation (SPD). It

* Corresponding author. Tel.: +81-22 215 2068; fax: +81-22 215 2066.
E-mail address: nita@imr.edu (N. Nita).

0022-3115/$ - see front matter © 2004 Elsevier B.V. All rights reserved.
doi:10.1016/j.jnucmat.2004.04.058

consists of an equal channel angular pressing (ECAP) followed by 6 GPa and 5 turns of high pressure torsion (HPT) [6]. In addition, electro deposited Ni (ED Ni) provided by Goodfellow Cambridge Ltd. [7] was considered. Densities of the samples were measured by Archimedes principle with a microgram balance. Almost full densities (>99%) without porosity were obtained in all samples.

Irradiation experiments were conducted in the Proton IRradiation EXperiment facility (PIREX) located at the Paul Scherrer Institut in Switzerland [8] and in the Tandem type accelerator at the Swiss Federal Institute of Technology Zurich (ETHZ). TEM discs with a diameter of 1 mm were punched out from 8 mm disc of SPD samples and irradiated in PIREX with 590 MeV protons at room temperature. Damage levels were 0.56 dpa for Ni and 0.91 dpa for Cu–0.5A_2O_3. Damage rates were about 1.5×10^{-6} dpa s^{-1}. Three millimeter TEM discs of ED Ni were punched out from the sheet of 0.2 mm thickness, electro polished to thin foil for TEM observation and then irradiated in a Tandem type accelerator with Ni^+ ions of 840 keV at room temperature. Damage levels were from 0.0005 to 5 dpa with the damage rates of 1×10^{-5} to 1×10^{-3} dpa s^{-1}.

X-ray diffraction spectrometry (XRD) was performed with a Siemens D500 X-ray diffractometer to obtain the average grain size and lattice strain of the unirradiated samples. Grain sizes were calculated from the broadening of peaks using family planes of {1 1 1}/{2 2 2} and {2 0 0}/{4 0 0}, which is based on the Scherrer formula [9]. The discs were jet-electro polished prior to TEM observation with electrolytes containing 12% H_2SO_4 and 88% CH_3OH at 0 °C with 15 V, and 25% H_3PO_4, 50% H_2O and 25% C_2H_5OH at room temperature with 15 V, for Ni and Cu–0.5A_2O_3, respectively. TEM observations were carried out with a JOEL 2010 operated at 200 kV. The foil thickness was determined by the convergent beam diffraction (CBD) technique. In-situ isochronal annealing observations up to 350 °C were also performed using a heating double tilt holder. The thermal stability of A_2O_3 particles in Cu–0.5A_2O_3 was examined after annealing experiments by energy dispersive X-ray spectrometer (EDS).

3. Results

3.1. Microstructure of SPD Ni

Fig. 1 shows the microstructure of SPD Ni. Random oriented grains are observed in both unirradiated and irradiated sample. Sub-grains are observed in grains with sizes larger than about 200 nm in unirradiated material. Highly strained regions are observed in irradiated sample. A selected area diffraction pattern confirms the expected ring pattern for the ultra fine-grained

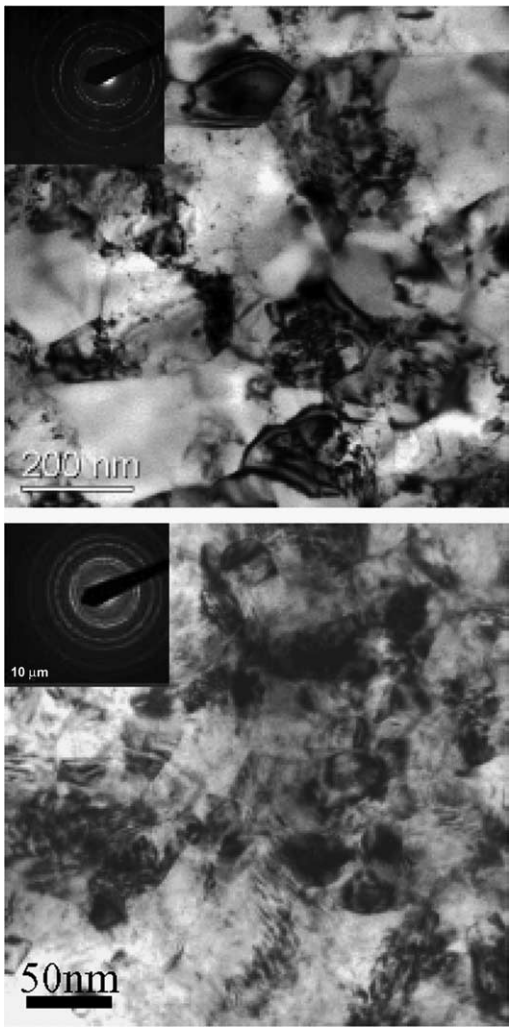

Fig. 1. The microstructure of SPD Ni in both unirradiated (top) and irradiated (bottom) sample. Note that the scales are different.

FCC materials. Continuity of the rings appears more complete in the irradiated material, indicating that a larger number of smaller grains were in the selected area. The average grain size decreases from 115 to 38 nm following proton irradiation to 0.56 dpa. It should be noted that a mean grain size of 34 nm was measured by XRD experiment in the unirradiated material. Although no specific measurement for the size distribution of sub-grains was done by TEM, this value corresponds to the sub-grains observed in TEM. Stacking fault tetrahedra (SFT) are observed in the irradiated material as well as twin boundaries that are parallel to {1 1 1} plane. Twin boundaries are also observed in unirradiated sample but in a lower number density. The number density of SFT is 7.4×10^{22} m^{-3} with a mean size of 2.5 nm.

3.2. Microstructure of SPD Cu–0.5A_2O_3

In SPD Cu–0.5A_2O_3, the typical randomly oriented nanocrystalline microstructure was observed in both unirradiated and irradiated materials. Fig. 2 shows the distribution of grain size in SPD Cu–0.5A_2O_3. Contrary to SPD Ni, Cu–0.5A_2O_3 exhibits grain growth as a consequence of irradiation. Average grain size increased from 178 to 493 nm following proton irradiation to 0.91 dpa. SFT and a low density of dislocations are observed in the irradiated Cu–0.5A_2O_3. The number density of SFT was 1.0×10^{22} m^{-3} with a mean size of 4.4 nm. Larger size of cascade and lower stacking fault energy of Cu explains that the value was larger than the size of SFT in Ni [10]. But this is the first time that SFT which is larger than 2 nm are observed after irradiation.

3.3. Microstructure of ED Ni

Fig. 3 shows the microstructure of ED Ni unirradiated and irradiated with Ni^+ ions. The average grain size is about 30 and 20 nm as deduced by TEM and XRD, respectively. Remarkable changes of the size and morphology do not occur following irradiation, although a small change of the shape is observable after 0.005 dpa. Surface contamination in the form of oxide is observed on irradiated specimens. As of radiation-induced defects, SFT are observed in the grains of irradiated samples after 0.5 dpa, while cavities or interstitial loops are absent.

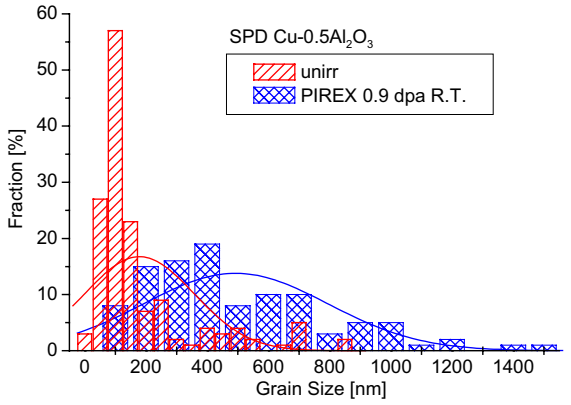

Fig. 2. The grain size distribution of both unirradiated and irradiated sample in SPD Cu–0.5Al_2O_3.

4. Discussion

4.1. Density of defects in grain

Microstructures exhibiting only SFT, without interstitial loops, are observed in irradiated nanocrystalline materials. It is concluded that a large fraction of grain boundary act indeed as an efficient sink for mobile defects, similarly to what was found by MD simulations [4]. Number densities of SFT in nickel and copper as the function of damage are plotted in Fig. 4. Density of SFT in nanocrystalline materials irradiated by both protons and ions is smaller than that of coarsed grain sized materials [11–15]. It suggests a good resistance to irradiation of nanocrystalline materials.

4.2. Change in grain size

Change in grain size occurs in SPD Ni and SPD Cu–0.5A_2O_3 following PIREX irradiation with opposite tendency, namely, grain refinement in Ni and grain growth in Cu–0.5A_2O_3.

Annealing during irradiation may explain the change in grain size. Fig. 5 shows the microstructure of ED Ni and SPD Cu–0.5A_2O_3 annealed in TEM up to 350 °C. There is no significant change in size and morphology of grain up to 150 °C in both materials. Although the diffraction conditions are slightly changed during

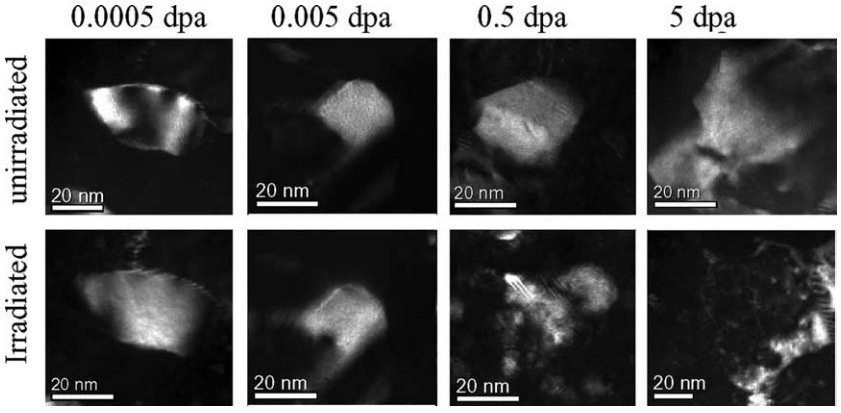

Fig. 3. The microstructure of ED Ni unirradiated and irradiated by Ni^+ ions up to 5 dpa.

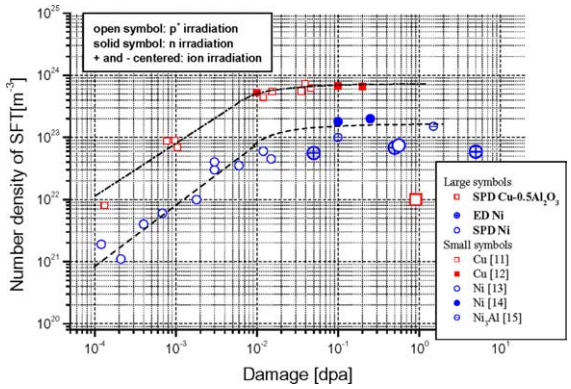

Fig. 4. Number densities of SFT in nickel and copper as the function of dose.

annealing, the grain growth is clearly observed after 300 °C in ED Ni and 200 °C in SPD Cu–0.5A_2O_3. Discontinuity of the rings in the diffraction pattern in both materials also indicates grain growth at elevated temperatures. The grain growth in Cu–0.5A_2O_3 starts at lower temperature and the grain size change rate is much faster than in Ni, which is explained by the fact that the melting point of Cu is lower than the one of Ni. The A_2O_3 particles, which are identified by EDS, remain unchanged even after annealing at 350 °C. The size of these particles is about 300 nm, which is larger than the grain size, and no finer particles, supposedly for the reinforcement of grain boundaries, have been observed in this study.

Grain growth in SPD Cu–0.5A_2O_3 by annealing can be excluded because the irradiation temperatures were below 100 °C in this study. But there still exists the possibility that irradiation enhanced the grain growth in Cu–0.5A_2O_3 as it is a thermally activated process, while in Ni the irradiation temperature, below 100 °C, is much too low to envisage such a process. Some researchers also reported grain growth in nanocrystalline thin foil following irradiation [16,17]. They concluded that the grain growth is due to enhancement of grain boundary mobility by irradiation or diffusion in the cascade volume during thermal spike. This mechanism could be adapted to the grain growth in SPD Cu–0.5A_2O_3, as the cascade volume is large enough [10].

One possible mechanism for grain refinement is that defect clusters produced by irradiation migrate to subgrain boundaries and form a cell structure that eventually may result in the formation of new smaller grains. Another possible mechanism for refinement of grains was reported by computational work [4]. They suggest that a cascade that is larger than the grain size forms a stacking fault across the grain, breaking the grain into two separate crystalline entities, thus leading to grain refinement. In the present study, the size of the subcascades is about 17 nm for a 590 MeV proton irradiation [8]. Although the size of cascade is smaller than the average grain size of unirradiated SPD Ni, overlap of cascade could support this mechanism.

There was no change in grain size following ion irradiation even in the specimen irradiated to 5 dpa. Although there are many differences between proton and ion irradiation such as damage rate, bulk or thin foil irradiation, 840 keV ion irradiation induces 12 nm of cascade which is smaller than the mean grain size of ED Ni. No evidence of change in grain size, such as stacking

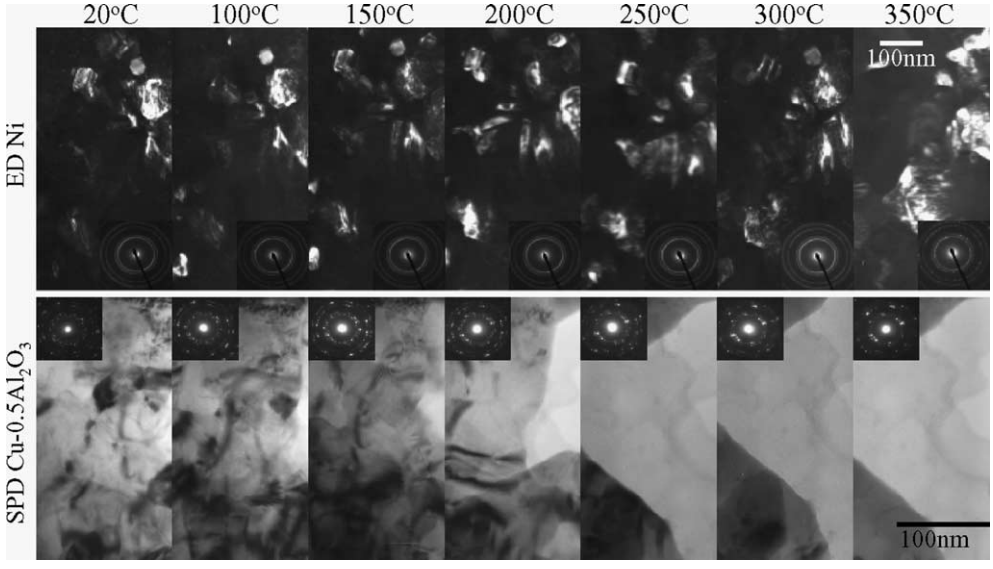

Fig. 5. The microstructure of ED Ni and SPD Cu–0.5Al_2O_3 annealed up to 350 °C.

fault across the grain for grain growth or accumulation of defect clusters for cell structure was observed following ion irradiation.

5. Conclusion

Irradiation experiments were performed in nanocrystalline Ni and Cu–0.5A_2O_3 by 590 MeV protons and 840 keV self ions. No defects except SFT were induced in nanocrystalline materials and density of SFT was smaller than normal-grained materials, which supports the idea of a good resistance against irradiation. Grain growth in SPD Cu–0.5A_2O_3 and refinement of grain in SPD Ni occurred by proton irradiation, while no change in grain size was observed in ED Ni irradiated by ions. According to annealing experiments, it appears that grain growth starts at 200 and 300 °C in Cu–0.5A_2O_3 and Ni, respectively.

Acknowledgements

The authors are grateful to IMR and PSI for the use of the facilities, Dr R. Z. Valiev for SPD samples and Dr M. Doebeli for ion irradiation at ETHZ. The authors would like to thank Drs H. V. Swygenhoven and F. Dalla Torre for valuable discussion.

References

[1] H. Gleiter, Prog. Mater. Sci. 33 (1989) 223.
[2] M. Rose, A.G. Balogh, H. Hahn, Nucl. Instrum. and Meth. B 127&128 (1997) 119.
[3] Y. Chimi, A. Iwase, N. Ishikawa, M. Kobiyama, T. Inami, S. Okuda, J. Nucl. Mater. 297 (2001) 355.
[4] M. Samaras, P.M. Derlet, H.V. Swygenhoven, M. Victoria, Phys. Rev. Lett. 88 (2002) 12.
[5] M. Besterci, J. Ivan, L. Kovac, Mater. Lett. 46 (2000) 181.
[6] R.Z. Valiev, R.K. Islamigaliev, I.V. Alexandrov, Prog. Mater. Sci. 45 (2000) 103.
[7] S. Shriram, S. Mohan, N.G. Renganathan, R. Venkatachalam, Trans. IMF 78 (2000) 194.
[8] P. Marmy, M. Daum, D. Gavillet, S. Green, W.V. Green, F. Hegedus, S. Proennecke, U. Rohrer, U. Stiefel, M. Victoria, Nucl. Instrum. and Meth. B 47 (1990) 37.
[9] B.E. Warren, B.L. Averbach, J. Appl. Phys. 21 (1950) 595.
[10] M. Alurralde, A. Caro, M. Victoria, J. Nucl. Mater. 183 (1991) 33.
[11] Y. Dai, D. Gavillet, F. Paschoud, M. Victoria, J. Nucl. Mater. 215 (1994) 393.
[12] B.N. Singh, Radiat. Eff. Def. 148 (1999) 383.
[13] M. Kiritani, Sci. Rep. Res. Tohoku A 45 (1997) 83.
[14] S.J. Zinkle, L.L. Snead, J. Nucl. Mater. 225 (1995) 123.
[15] P. de Almeida, M. Victoria, J. Phys. D Appl. Phys. 35 (2002) 2032.
[16] N. Karpe, J. Bottiger, N.G. Chechenin, J.P. Krog, Mater. Sci. Eng. A 179&180 (1994) 582.
[17] A.M. Ibrahim, Nucl. Instrum. and Meth. B 29 (1988) 650.